Sharp-Line Self-Induced Transparency

H. M. Gibbs and R. E. Slusher
Bell Telephone Laboratories, Murray Hill, New Jersey 07974
(Received 24 July 1972)

Self-induced transparency (SIT) has been observed under the conditions of sharp-line absorption, i.e., with an inhomogeneous absorption width only one-fourth the spectral width of the pulse. A 5-nsec pulse from a ^{202}Hg II laser intersected perpendicularly an atomic beam of natural rubidium. The beam slits reduced the Doppler absorption width to about 30 MHz. A particular resolved M_I transition of ^{85}Rb was scanned into coincidence with the laser pulse by a 75-kOe magnetic field. With peak absorption depths of 3–6, nonlinear transmission, pulse delays, pulse breakup, and peak amplification were seen and found to be in excellent agreement with sharp-line computer solutions of the Maxwell–Bloch equations. The experimental realization of the sharp-line SIT is of interest because analytical formulas for pulse evolutions are more plentiful and because sharp-line SIT might permit compression of picosecond pulses.

I. INTRODUCTION

Self-induced transparency[1] (SIT) in an absorber with inhomogeneous width much broader (≈ ten times in Hg-Rb experiment[2]) than the frequency spread of the pulse has been studied extensively yielding good agreement between theory and experiment.[1,2] The present paper is a study of sharp-line SIT in which the inhomogeneous Doppler width arising from thermal motion is reduced to about one-fourth the frequency spread of the pulse.[2(c)] This is accomplished by irradiating an atomic beam of Rb with an optical-pulse incident normal to the plane of the beam.

A 2π hyperbolic secant traveling-wave pulse is a unique analytical steady-state solution of the coupled Maxwell and Schrödinger equations in the sharp-line limit.[1] Lamb has also obtained an analytical solution for a 4π pulse which splits in its passage through a sharp-line absorber.[3] The fact that, in general, the analytical treatment of pulse evolution is much simpler for sharp-line than for broad-line absorption increases the interest in an experimental sharp-line system as reported here.[4] But in agreement with earlier computer analyses[5] no marked differences have been observed between broad- and sharp-line SIT. In particular, nonlinear transmission, pulse delays, pulse breakup, and peak amplification are all observed in the sharp-line case too. However, the peak absorption must be higher in the sharp-line case to yield similar output pulse shapes.

The outline of this paper is as follows. The apparatus is presented in Sec. II with an emphasis on the changes made in the Hg-Rb broad-line apparatus.[2] The experimental observations presented in Sec. III include narrow absorption profiles and typical sharp-line SIT pulse shapes. A comparison of the data with a computer simulation is drawn in Sec. IV along with a comparison of broad- and sharp-line SIT. The effect of losses on the stabilities of broad- and sharp-line SIT is discussed in Sec. V. The possibility of reshaping and compressing picosecond pulses is treated in Sec. VI. Conclusions and possible extensions of this work are given in Sec. VII.

II. APPARATUS

Much of the apparatus has been described in detail previously.[2] A 5–10-nsec coherent optical pulse was obtained from the 1-μsec output of a ^{202}Hg II laser by a Pockels-cell shutter. The TEM_{00} output was focused by a 38-cm lens to a 120-μm-diam focal region much longer than the sample at its center. The sample output was imaged by a 15-cm lens upon a 200-μm aperture which selected out the central portion of the transverse profile to approximate a uniform plane-wave condition. The temporal evolution of the output was monitored by a model No. TIXL 59 silicon avalanche photodiode and a 75-psec rise-time sampling oscilloscope. The Rb samples were situated in the ≈75 kOe magnetic field of a superconducting solenoid. The primary alterations in the broad-line apparatus[2] were: (i) replacing the ^{87}Rb absorption cell by an atomic beam of natural Rb; (ii) locking the long laser cavity to the short single-longitudinal-mode-selector cavity; and (iii) concurrently monitoring the pulse shapes and absorption coefficients.

The atomic beam of Rb was produced by a stainless-steel oven with a sidearm. The sidearm consisted of a Cu-constantan thermocouple and an American Standard model No. BXA06-B12-06M heater soldered to a 6-mm-i.d. stainless-steel tube with screw-in bottom plug. A 5-mm-o.d. Pyrex vial containing Rb metal was broken under xylene and inserted into the sidearm with a few millimeters

of xylene preventing oxidation of the Rb. The Rb contained in the vial was about 3 cm long and 3 mm in diam and usually lasted less than 30 min at the typical sidearm temperatures of 260–300 °C (controlled by an API Instruments model No. 226 temperature controller). A second American Standard heater was used to maintain the oven at least 20 °C hotter than the sidearm to prevent clogging of the slit. A simple screw-on plate pressed the slit sheet against the oven face. The slits used were 0.2 or 0.5 mm in height and were photoetched in 25-μm-thick molybdenum. The 1.2-cm-long beam slit was about 1 cm from the 0.65-cm-long oven slit; this small spacing was necessitated by the small diameter of the high-field region. The oven and its slit could be raised about 1 cm relative to the fixed beam slit by a micrometer screw. This permitted minimization of the Doppler profile in one plane. The atomic and light beams were made perpendicular in the other plane by adjusting the angle of incidence of the laser beam upon the atomic beam. The atomic beam could be stopped by a beam flag before reaching the region of interaction with the laser beam. Alcohol was circulated through an alcohol–dry-ice mixture (≈ -70 °C) and through a Cu block to which the beam slit was attached. The Rb emitted by the oven stuck to this cold block and did not reenter the beam. Without the circulation of this coolant a broad asymmetric absorption spectral profile was seen. Also, reduced absorption was seen if the oven slit or sidearm plug permitted Rb to escape the oven without going through the oven slit. Typical pressures at the vacuum station used to evacuate the beam-slit insert were 10^{-5} T or less.

For single-longitudinal-mode operation, the frequency of one mode of the long cavity must coincide with the frequency of the mode of the short single-mode-selector (SMS) cavity which lies within the gain curve of the lasing medium.[2] In earlier SIT experiments this was accomplished by changing the length of the SMS cavity so that the SMS mode coincided with the long-cavity mode closest to the desired operating frequency. A manually operated piezoelectric crystal made this possible. In the present experiment a 2.5-Hz modulation was applied to that crystal to produce an error signal which was detected by a model No. PAR 160 boxcar and model No. HR-8 lock-in amplifier, amplified by a Kepco model No. OPS-2000 operational amplifier, and applied to a Coherent Optics (now Spectra) model No. 560 piezoelectric translator to which the 3-m-long cavity mirror was affixed. This feedback system with a response time of about 1 min was adequate to compensate for thermal and mechanical long-cavity length changes. The SMS cavity ran freely, its frequency being periodically set at the center of the beam absorption.

Because absorption depths of 3–5 are needed to observe SIT and because the space limitations and sharp-line criterion results in narrow slits, the operating time for each Rb vial was only 20–30 min before slit clogging or sample depletion eliminated the absorption. Gradual heating of the oven and sidearm to prevent excessive outgassing also introduced a time dependence to the absorption coefficient. To optimize the utilization of the operating time a scheme was devised to observe the pulse shapes and absorption concurrently. The laser was operated at 160 pulses per sec but the Pockels cell was opened for 5 nsec only every other laser pulse. During the other half of the laser pulses a synchronized model No. PAR 222 variable speed chopper inserted (at the laser output) a linear polarizer with transmission axis at 45° to the laser polarization and to the Pockels-cell-shutter exit polarizer. This permitted part of the long pulse to pass the shutter. The chopper also inserted a neutral-density filter to reduce the long-pulse intensity into the linear regime. An Amperex model No. 56TVP, PAR CW-1 boxcar, and recorder sufficed to monitor the transmission of this long pulse through the atomic beam. Of course, the boxcar was triggered only on alternate laser pulses when the Pockels-cell shutter was not triggered. This concurrent measurement of αL and pulse shape made possible the acquisition of useful data as αL increased with heating and decreased with clogging or depletion.

III. OBSERVATIONS

A. Absorption Profile with Reduced Doppler Width

For most of the data the oven slit was 0.2×6.5 mm and the beam slit 0.5×12.7 mm. The absorption profiles for the long and short pulses are displayed in Fig. 1. The 30-MHz long-pulse absorption width is in good agreement with that expected from a simple geometric and gas kinetic calculation. In theory, a 5-nsec Gaussian pulse has an 88-MHz Gaussian spectral profile which is three times the observed beam absorption width. Subtraction of the 30-MHz beam width from the ≈ 150-MHz long-pulse width observed yields about 120 MHz or four times the beam width. The short-pulse absorption measurement was made using the entire short pulse including succeeding secondary pulses arising from electrical mismatch. The more nearly trapezoidal rather than Gaussian shape of the input pulse also contributed to the ≈ 120-MHz short-pulse width. The ratio of pulse-frequency width to beam-absorption width was then about four and certainly no less than three. The conditions for a sharp-line experiment were thus satisfied. The narrow long-pulse absorption profile was shifted and broadened by translating the

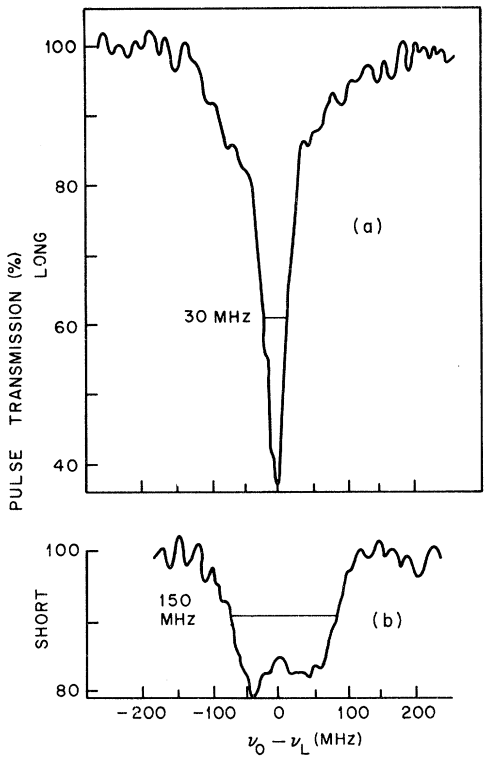

FIG. 1. Percentage transmission of the (a) long (1 μsec) and (b) short ($\approx$ 5 nsec) optical pulses through the Rb atomic beam defined by a 0.5 × 12-mm beam slit 1 cm from the 0.2 × 6.5-mm oven slit. The optical pulse center frequency ν_L was held fixed while the center frequency ν_0 of the beam absorption was scanned via the external magnetic field. The half-widths refer to the absorption coefficient αL, not to the observed transmission which is related to αL by $I = I_0 e^{-\alpha L}$; it was assumed that the profiles were Gaussian since the reduced Doppler width was still about five times the natural radiative width. The long-pulse peak αL in (a) is about 1 corresponding to a sidearm temperature of about 220 °C. Similar widths were seen for higher αL's. The absorption curves shown here are for the resolved ^{85}Rb $M_I = \frac{1}{2}$ component of the natural Rb absorption in the neighborhood of 75 kOe.

beam oven and thereby increasing the observed Doppler shifts. The ease with which isotope shifts could be measured with an atomic beam and stable laser is illustrated by Fig. 2. Those data were taken to choose a resolved line for studying sharp-line SIT (^{85}Rb, $M_I = \frac{1}{2}$ was chosen); it was noticed later that they contain information from which the isotope shift can be deduced. Clearly much more precise measurements could be made.[6]

B. Sharp-Line SIT Pulse Shapes

SIT pulse shapes were studied in the sharp-line case by varying the input intensity and recording the input and output pulses with a sampling oscilloscope.[2] Figures 3(a) and 4 present representative data for sharp-line SIT in which the pulse-frequency width was three to six times the inhomogeneous absorption width. The long-pulse transmission was measured concurrently with the recording of the pulse shapes to verify the constancy of the αL. The characteristic features of broad-line SIT are seen to be present in the sharp-line case as well.

IV. COMPARISON WITH THEORY

The spectral linewidth for the experiments described here [$\Delta\nu \simeq 30$ MHz, full width at half-maximum (FWHM)] is still wider than the homogeneous linewidth caused by spontaneous decay from the excited state,[2] i.e., the homogeneous width is

$$\Delta\nu_H = \frac{1}{2\pi}\left(\frac{1}{\tau_{ab}} + \frac{1}{\tau_{ac}}\right) \quad (1)$$

$$= \frac{1}{2\pi}\left(\frac{2}{T_2'}\right) \quad (2)$$

$$\simeq 5.7 \text{ MHz (FWHM)},$$

where τ_{ab} and τ_{ac} are the decay times from excited to ground state and excited state to the upper-Zeeman-branch ground state, and T_2' is the transverse relaxation time. However, since the inhomogeneous Doppler broadening of 30 MHz is small compared to the 120-MHz Fourier transform of the input pulse, the results obtained here are expected to be similar to the homogeneous sharp-line case at least for times less than $1/\pi\Delta\nu_D \simeq 10$ nsec. McCall and Hahn[1] have obtained unique analytical solutions for a sharp-line absorber (homogeneous or inhomogeneous). The stable solutions have an area

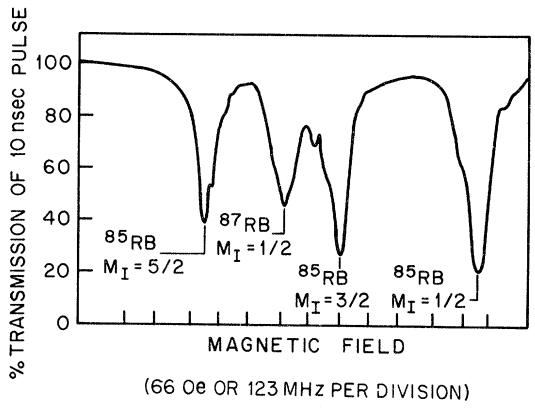

FIG. 2. Transmission of a 10-nsec 7944.5-Å pulse through a beam of natural Rb as a function of magnetic field ($\approx$ 125 MHz/division) in the vicinity of 75 kOe. The ^{85}Rb absorption dips are not equal because the beam density was not constant. The ^{87}Rb-^{85}Rb isotope shift can be deduced from these data and known hyperfine coupling constants.

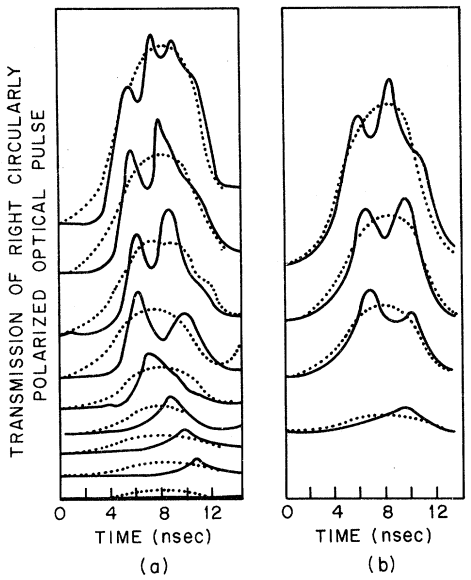

FIG. 3. Sharp-line SIT pulse shapes. (a) Experimental pulse shapes; dotted curves are the inputs taken by inserting the beam flag; solid curves are the outputs after passage through the Rb atomic beam. The absorption width was 30 ± 5 MHz, and the peak αL was 6 ± 1. This is a lower limit for αL since some of the unabsorbed light may have had the wrong polarization. The 5-nsec-pulse Fourier transform was four times broader than the absorption width, and the maximum effective αL was reduced to 1.5. The Rb sidearm temperature was 300 °C. The oven slit (0.2×6.5 mm) was 1 cm from the beam slit (0.5×12.7 mm). (b) Computer simulations of experiment from simultaneous solution of Maxwell and Bloch equations. Input pulses (areas 2π, 4π, 5π, and 6π) are drawn as dotted curves. Input-pulse shapes were taken from the corresponding experimental pulses in (a). Computed output pulses are shown as solid curves assuming $\alpha L = 6$, $T_1 = 33.6$ nsec, $T_2 = 56$ nsec, and absorber Doppler width of 30 MHz. The greater depth of the pulse-breakup dips and the heavier absorption on the leading edge in (a) than in (b) suggest that the experimental αL was closer to 10 (see Fig. 5).

$$A = (2p/\hbar) \int_{-\infty}^{\infty} \mathcal{E}(z, t)\, dt = 2\pi \,, \tag{3}$$

where p is the electric dipole moment of the resonant transition, $\mathcal{E}$ is the envelope of the pulse electric field, and

$$\mathcal{E}(z, t) = \frac{2}{\kappa\tau} \operatorname{sech}\left[\frac{1}{\tau}\left(t - \frac{z}{V_{SH}}\right)\right] \,, \tag{4}$$

where

$$\frac{1}{V_{SH}} = \frac{\alpha\tau}{2}\left(\frac{\tau}{T_2'}\right) + \frac{\eta}{c} \,, \tag{5}$$

τ is the pulse width, and V_{SH}^{-1} the delay time per cm for a sharp homogeneous absorber ($\tau_p < T_1$, $T_2' < T_2^*$). Equation (5) is obtained using $1/V_{SH}$ from Eq. (44) of Ref. 1,

$$\alpha = 8\pi^2 N p^2 \omega g(0)/\eta\hbar c \tag{6}$$

and a Lorentz line shape,

$$g(\Delta\omega) = T_2'/\pi[1 + (\Delta\omega T_2')^2] \,. \tag{7}$$

For a sharp-line inhomogeneous absorber ($\tau_p < T_2^* < T_1$, T_2'), the τ/T_2' factor in Eq. (5) is replaced by a factor of the order of τ/T_2^* which depends on the exact line shape. It is interesting to compare this to the delay time per cm for a broad inhomogeneous absorber,[1] i.e.,

$$(1/V_{BI}) = \tfrac{1}{2}\alpha\tau + \eta/c \,. \tag{8}$$

For $\alpha\tau^2/T_2' \gg \eta/c$ and $\alpha\tau \gg \eta/c$ (usually the case of interest),

$$V_{BI}/V_{SH} = \tau/T_2' < 1 \,, \tag{9}$$

since $\tau < T_2'$ must obtain for coherent propagation. The velocity is faster for the sharp-line case, because the pulse has many spectral components outside the absorption width. Thus the effective absorption is reduced by the ratio of the absorption width ($\propto 1/T_2'$) to the pulse-frequency width ($\propto 1/\tau$), i.e.,

$$\alpha_{eff} = \alpha\tau/T_2' \tag{10}$$

for the homogeneous sharp-line case, where α is the absorption measured for a cw optical beam (or pulse width $\tau \gg T_2'$) at the center of the absorption line. For the sharp-line inhomogeneously broadened case of interest for the experiments described here,

$$\alpha_{eff} \approx \alpha\tau/T_2^* \,. \tag{11}$$

Then in general Eq. (8) gives the velocity provided α is replaced by the appropriate α_{eff}.

Computer solutions similar to those in Ref. 2

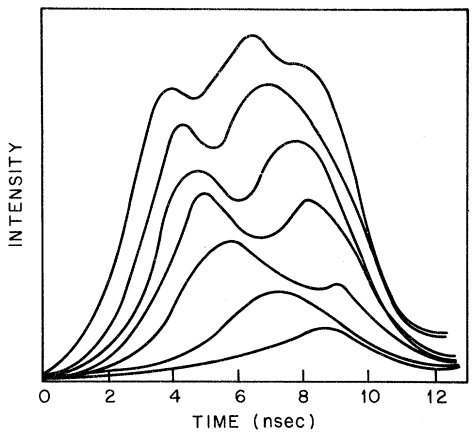

FIG. 4. Sharp-line SIT output-pulse shapes for input areas in the range 2π to 6π. Long-pulse absorption width was 20 ± 5 MHz with peak $\alpha L = 2.75 \pm 0.5$. Both the oven and beam slits were 0.2 mm high.

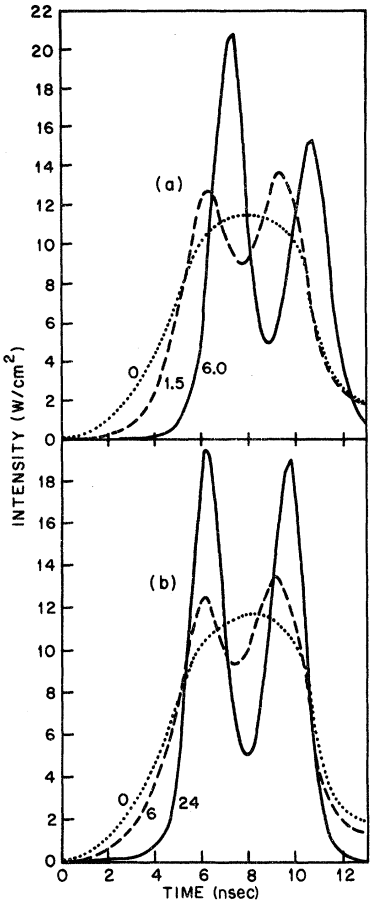

FIG. 5. Comparison of SIT for sharp- and broad-line absorbers. Dotted trace in (a) and (b) is a replica of an experimental input pulse whose Fourier transform is 120 MHz. Pulse evolution for a 5π pulse in a 566-MHz Doppler-broadened inhomogeneous absorber is shown in (a). Numbers beside dashed and solid curves indicate the peak αL. An identical input pulse evolving in a 30-MHz Doppler-broadened absorber is shown in (b). Relaxation times of $T_1 = 67.2$ nsec and $T_2' = 112$ nsec were used for these computations (computer simulation).

were used to simulate the experiments shown in Fig. 3(a) for the sharp Rb absorber. Bloch's equations[2] are

$$\dot{u} = v\Delta\omega - u/T_2' , \tag{12}$$

$$\dot{v} = -u\Delta\omega - \kappa^2 \mathcal{E} W/\omega - v/T_2' , \tag{13}$$

$$\dot{w} = v\mathcal{E}\omega - (x+W)/T_1 , \tag{14}$$

$$\dot{x} = -(2/T_2' - 1/T_1)(x+W) , \tag{15}$$

where

$$x = \tfrac{1}{2}N\hbar\omega_0 \langle I \rangle , \tag{16}$$

the transverse components of polarization are defined by

$$u + iv = \tfrac{1}{2}Np \langle \sigma_x + i\sigma_y \rangle , \tag{17}$$

and the energy is

$$W = \tfrac{1}{2}N\hbar\omega_0 \langle \sigma_z \rangle . \tag{18}$$

The incoherent longitudinal and transverse relaxation rates are, respectively,

$$\frac{1}{T_1} = \frac{1}{2\tau_{ac}} + \frac{1}{\tau_{ab}} = (33.6 \text{ nsec})^{-1} \tag{19}$$

and

$$\frac{1}{T_2'} = \frac{1}{2\tau_{ac}} + \frac{1}{2\tau_{ab}} = (56 \text{ nsec})^{-1} , \tag{20}$$

where τ_{ab} and τ_{ac} are the decay times from the excited state $|a\rangle$ to states $|b\rangle$ and $|c\rangle$ [see Ref. 2(b)]. Equations (12)–(15) were solved simultaneously with Maxwell's equation,

$$\frac{\partial \mathcal{E}}{\partial z} + \frac{1}{c}\frac{\partial \mathcal{E}}{\partial t} = \frac{-2\pi\omega}{c}\int_{-\infty}^{\infty} g(\Delta\omega)\, v(\Delta\omega, z, t)\, d(\Delta\omega) , \tag{21}$$

using the narrow Doppler profile for $g(\Delta\omega)$ with $\Delta\nu_D = 30$ MHz. The computer integration included T_1 and T_2' processes and was performed as described in Ref. 2(b). There were 50 computed intervals in αL, where α was the line-center absorption constant and L was the sample length. There were also 50 time and $\Delta\omega$ intervals chosen as described in Ref. 2(b). Experimental pulse envelopes were used as initial computer electric fields. Computer output pulses are shown in Fig. 3(b) adjacent to the corresponding experimental output pulses. Agreement between computed and experimental output pulse shapes is good. Both experimental and computed outputs show pulse breakup at 4π and 6π with similar pulse delays and shapes. The effective absorption length is only $\alpha_{eff} L \approx 1.5 = 6 \times (30 \text{ MHz}/120 \text{ MHz})$ for results shown in Fig. 3; thus the pulses are expected to still be evolving to their stable 2π hyperbolic secant forms, and pulse separation in the 4π and 6π regions is not yet complete.

A comparison of computed results for the broad (a) and sharp (b) inhomogeneous absorbers is shown in Fig. 5. Initial conditions are again similar to those used experimentally in Fig. 3(a) and in Ref. 2 (T_1 and T_2' decays are included). As shown above, the effective absorption constant is reduced for the sharp-line absorber. Other than the effective change in α, the only difference in the pulse breakup and shapes for the 5π input pulses shown in Fig. 5 seems to be a difference in the relative intensities and delays of the two pulses (each is evolving toward 2π). Pulse delays are less for the sharp-line case. This may be related to the relatively sharp rise time of the experimental input pulse. Note that at low intensities on the leading edge of the pulse there is significantly more transmission in the sharp-line than in the broad-line

absorber. This is expected because the Fourier components of the fast rising pulse lie beyond the 30-MHz sharp-line-absorber width.

V. STABILITY AND INCOHERENT LOSSES IN BROAD- AND SHARP-LINE LIMITS

For the broad inhomogeneous absorber it has been shown that input-pulse areas between π and 3π evolve to the stable 2π area with hyperbolic secant pulse shape and a velocity given by Eq. (8). This is easily proved for the inhomogeneous absorber because of the area theorem

$$\frac{dA(z)}{dz} = -\tfrac{1}{2}\alpha \sin A(z) , \tag{22}$$

where A is the pulse area defined by Eq. (3). The area-theorem derivation requires a time after the $\mathcal{E}$ field effects are negligible during which the polarization components at various $\Delta\omega$ can dephase at a rate $1/T_2^*$. This dephasing after the pulse must occur before T_1 and T_2' incoherent processes come into effect. In the present experiment the reduced inhomogeneous Doppler width of 30 MHz still dominates the 5.7-MHz-wide homogeneous profile arising from lifetime broadening. But the spectral width is still much narrower than the 120-MHz Fourier transform of the pulse. Thus, the area theorem does ensure evolution toward stable 2π pulses. However, since T_2^* is only a factor of 2 to 4 smaller than T_2', the region where the area theorem does not apply is being approached.

An interesting and useful way to estimate how far the 2π pulse will propagate in the absorber is to consider the energy loss caused by the inevitable incoherent decay processes. For Rb these decay processes can be included in the Bloch equations [Eqs. (12)–(15)]. Equation (15) is a measure of the loss of atoms from the excited two-level system ($|a\rangle$ and $|b\rangle$) to the third level ($|c\rangle$) by spontaneous decay. This loss rate to level $|c\rangle$ is quite small on a time scale of 10 nsec and can be neglected in first order, in which case Eqs. (12)–(15) reduce to Eqs. (24)–(26) of Ref. 1. McCall and Hahn estimated the energy loss of the propagating 2π pulse (see Sec. IV of Ref. 1). For the sharp-line case (homogeneous or inhomogeneous) they found to first order in τ/T_S,

$$\frac{d\mathcal{T}_S}{dz} = -\frac{4N\hbar\omega\tau}{3T_S} , \tag{23}$$

where the pulse energy per cm^2 is

$$\mathcal{T} = (c/4\pi)\int_{-\infty}^{\infty} \mathcal{E}(z,t)^2\,dt \tag{24}$$

and

$$\frac{1}{T_S} = \frac{2}{T_1} + \frac{1}{T_2'} = (12.9\ \text{nsec})^{-1} \tag{25}$$

for Rb. For the 2π hyperbolic secant transparency pulse of Eq. (4),

$$\mathcal{T} \approx 2c/\pi\kappa^2\tau , \tag{26}$$

permitting the expression of the z dependence of τ in terms of $\mathcal{T}$; Eq. (23) becomes

$$\frac{d\mathcal{T}_S}{dz} = -\frac{8N\hbar\omega c}{3\pi\kappa^2 T_S}\frac{1}{\mathcal{T}_S} . \tag{27}$$

For the inhomogeneous broad-line case they found

$$\frac{d\mathcal{T}_B}{dz} = -\frac{4\pi N\hbar\omega g(0)}{3T_B} , \tag{28}$$

where

$$\frac{1}{T_B} = \frac{1}{T_1} + \frac{2}{T_2'} = (15.2\ \text{nsec})^{-1} \tag{29}$$

for Rb.

In both sharp-line and broad inhomogeneous absorbers a 2π pulse loses energy and τ increases. Pierce and Hahn[7] have recently introduced an interesting way to characterize this decay of a 2π pulse in terms of a "critical length." At some critical distance, Z_S (or Z_B), τ will equal T_S (or T_B), and for larger distances into the absorber, the pulse will lose energy much more rapidly than predicted from Eqs. (27) and (28), since incoherent decay processes will dominate. Integrating (27) and using Eq. (26) with $\tau(Z_S) = T_S \ll \tau(0) = \tau_0$, one has for the sharp-line critical distance

$$Z_S = \frac{3g(0)\pi}{2\alpha}\frac{T_S}{\tau_0^2} , \tag{30}$$

which can be written

$$Z_S = \frac{3}{2\alpha_{\text{eff}}}\frac{T_S}{\tau_0} , \tag{31}$$

where α_{eff} is given by Eqs. (10) and (11) for the homogeneous and inhomogeneous case, respectively, with $\tau = \tau_0$. Similarly for the broad-line case,

$$Z_B = \frac{3T_B}{\alpha\tau_0} . \tag{32}$$

Pierce and Hahn[7] obtained an expression similar to Eq. (31) from computer calculations for the sharp-line case. They also found that the pulse area evolves toward 2π for $Z < Z_S$ for the sharp homogeneous absorber, in a way similar to the broad inhomogeneous absorber where the area theorem applies. Although only a first-order estimate, the critical distance Z is quite useful in determining how many absorption lengths αZ a stable 2π pulse will propagate before being destroyed by incoherent processes. Beyond Z the pulse will decay in a few absorption lengths. For the Rb absorber, Z is expected to be two or three times less for the sharp homogeneous absorber than for the broad

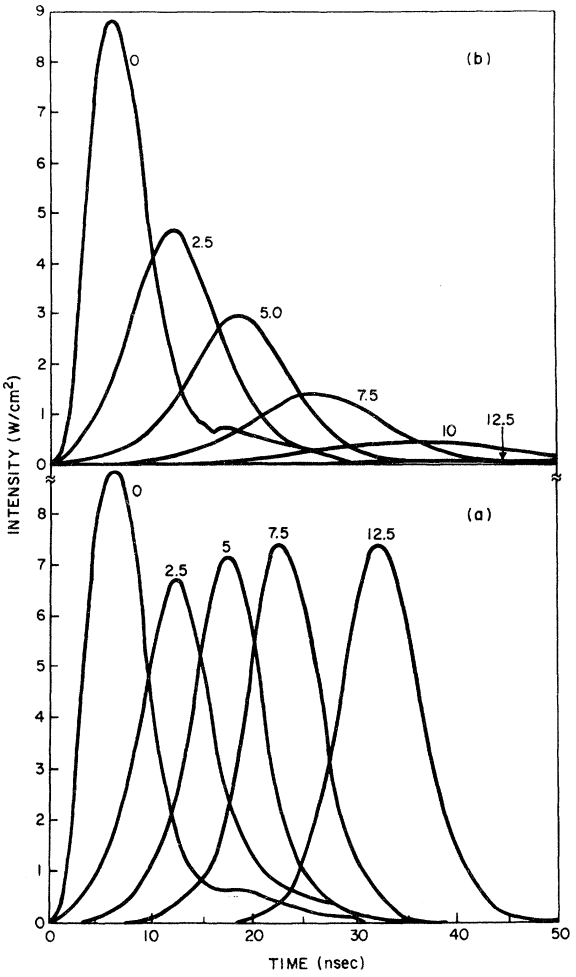

FIG. 6. Effect of T_1 and T_2' on pulse evolution for a broad-line absorber (computer simulation). The evolution of a 2π pulse with experimental input-pulse shape using computer solutions is shown with (b) and without (a) incoherent decay, T_1 and T_2'. Parameters are the following:

(a) $T_1 = 10\,000$ nsec, $T_2' = 20\,000$ nsec;

Area	αL	E_0/E_I
6.28	0	1.0
6.24	2.5	0.928
6.25	5.0	0.922
6.26	7.5	0.921
6.21	12.5	0.920

(b) $T_1 = 33.6$ nsec, $T_2' = 56$ nsec;

Area	αL	E_0/E_I
6.28	0	1.0
5.89	2.5	0.74
5.52	5.0	0.54
4.85	7.5	0.34
3.14	10.0	0.14
0.12	12.5	0.02

αL is labeled on each pulse.

inhomogeneous absorber (using α_{eff} for the sharp homogeneous absorber). For a typical input-pulse width of 3 nsec,

$$\alpha Z_B \simeq 3\,\tfrac{15.2}{3} \simeq 15.2 \tag{33}$$

for the broad inhomogeneous case and

$$\alpha Z_S \simeq \tfrac{3}{2}\,\tfrac{12.9}{3} \simeq 6.45 \tag{34}$$

for the sharp-line case. Both αZ's exceed the highest αL's used in the experiments described here and in Ref. 2 by about a factor of 3. In the broad-line experiment severe losses were observed for αL's of 10–15. Effective αL's higher than about two were not achieved for the sharp-line experiment because of limitations of atomic beam density.

The estimates for critical distance in Eqs. (31) and (32) can be compared with the more precise computer calculations for both broad- and sharp-line cases. Computer results for the broad-line case are repeated here in Fig. 6 (these results are the same as the corrected Fig. 4 of Ref. 2; see erratum to Ref. 2). For large T_1 and T_2', the pulse evolves into a 2π hyperbolic secant pulse propagating with a velocity given by Eq. (8). With the values of T_1 and T_2' obtained for Rb the pulse loses energy linearly with distance, the pulse broadens, but the area remains near 2π until $Z \approx Z_B$, the critical length predicted from Eq. (32). The decay of pulse energy and area as a function of distance in the absorber are plotted as solid lines in Fig. 7 for the broad-line case. Note the good agreement with both linearity of the energy decay and the critical distance predicted by Eqs.

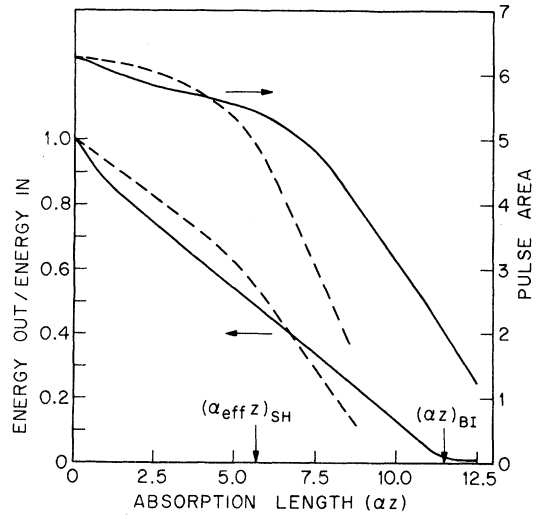

FIG. 7. Pulse area (upper curves) and energy (lower curves) as a function of distance into the absorber for broad-line (solid) and sharp-line (dashed) absorbers (computer simulation).

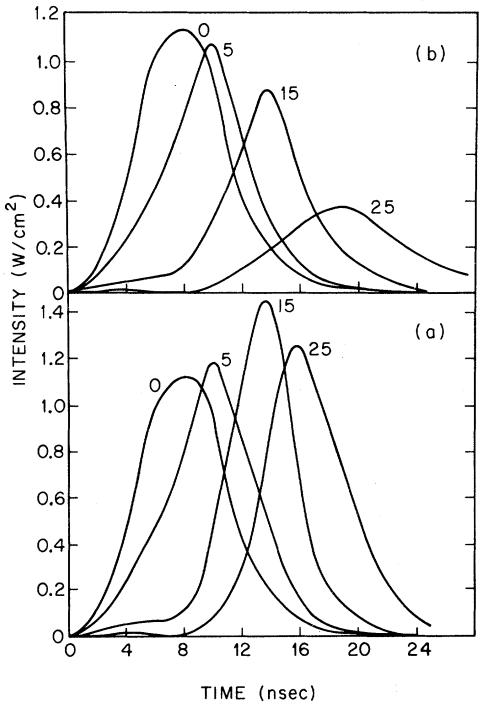

FIG. 8. Evolution of a 2π area input pulse with experimental pulse shape using computer solution with (b) and without (a) incoherent decay, T_1 and T_2'. Parameters are the following:

(a) $T_1 = 1000$ nsec, $T_2' = 1500$ nsec;

Area	αL	E_0/E_I
6.28	0	1.0
6.3	5	0.99
6.11	15	0.98
5.9	25	0.97

(b) $T_1 = 33.6$ nsec, $T_2' = 56$ nsec;

Area	αL	E_0/E_I
6.27	0	1.0
6.22	5	0.92
5.8	15	0.74
4.4	25	0.46

αL listed above and beside each curve is the αL for a weak cw beam at the center of the absorber spectrum; the effective αL for the pulse used here is four times smaller than this line center αL.

(31) and (32).

The sharp-line decay is shown in Fig. 8 using the same input pulse as in Fig. 3. Again without losses, the pulse evolves to a stable 2π hyperbolic secant pulse with velocity given by Eq. (8) using $\alpha = \alpha_{eff} = 1.5$. Note the narrowing of the pulse during reshaping; this reshaping depends strongly on the input-pulse shape (e.g., rise time, fall time, etc.). With the values of T_1 and T_2' appropriate for Rb the pulse evolution shown in Fig. 8(b) is obtained for the sharp-line conditions obtained in the experiments described here. The pulse decays in a distance of the same order as the broad-line case which is in reasonable agreement with Eqs. (33) and (34). The disagreement is probably caused by the initial pulse narrowing obtained for the experimental pulse shape used in Fig. 8. The decay of pulse energy and area are shown as dashed lines in Fig. 7. The energy does not decay linearly with distance as in the broad-line case [Eq. (28)]. This is because as the sharp-line pulse lengthens, the effective α increases. These computer simulations indicate that Z_B is an excellent estimate of the decay in the broad-line limit, and Z_S is an order-of-magnitude estimate because of the strong dependence on input-pulse shape.

VI. PULSE COMPRESSION AND SHAPING OF PICOSECOND PULSES

It will be very interesting to study the effects of picosecond pulses in the SIT regime. Chirping and envelope nonuniformity may cause interesting effects and higher-energy atomic levels may cause deviations[2(b)] from the simple SIT described here and in Refs. 1 and 2. For atomic absorbers similar to atomic Rb, the absorber linewidth may be

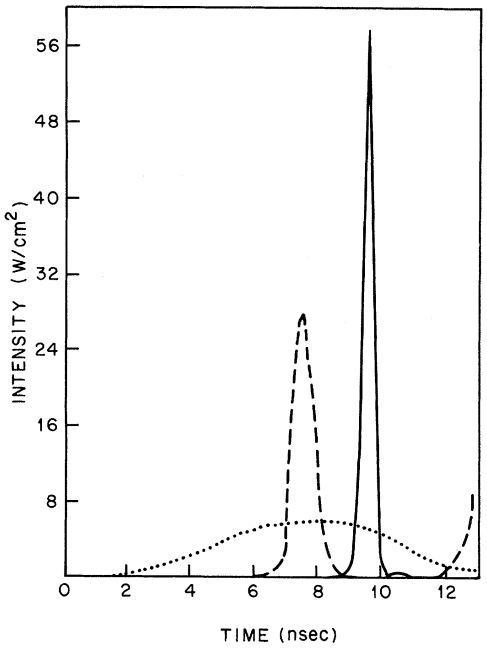

FIG. 9. Pulse narrowing by focusing in a sharp-line absorber. Dotted curve is input pulse with $A = 11 = 3.5\pi$. Solid curve shows effect of focusing in a broad inhomogeneously broadened absorber with $\alpha L = 25$. Dashed curve shows effect of a similar focusing experiment in a sharp-line absorber with peak $\alpha L = 100$ and $1/\Delta\nu_D T \approx 4$.

sharp (< 1 GHz) compared to the Fourier transform of a pulse in the 1–50-psec range ($\Delta\nu \approx 300$–6 GHz), and results obtained for the sharp-line case above should apply (if chirping, other atomic levels, etc., can be ignored). Pulse-envelope reshaping may be an important application of SIT in the picosecond range. In particular, it has been shown that for the broad inhomogeneous absorber, focusing a 3π pulse in an absorber can cause pulse compression by an order of magnitude.[8] In view of the possibility of compressing picosecond pulses, it is interesting to see if similar compression can be obtained for the sharp-line absorber. Figure 9 shows a computer calculation of pulse narrowing for both sharp and broad inhomogeneous absorbers. Input-pulse shapes and absorber linewidths are similar to those used in Figs. 3 and 5 (≈6 nsec FWHM pulse, ≈30 MHz linewidth) but should scale to apply for a 60-psec input pulse in a 3-GHz sharp-line absorber. Focusing in the sharp-line case is not as effective as in the broad-line case but is still in a useful range for pulse narrowing (≈ a factor-of-6 compression). These results are expected qualitatively, since as the pulse narrows its Fourier spectrum widens and the effective absorption constant decreases in the sharp-line case (remains constant in the broad-line limit) thus reducing the ability of the absorber to reshape the pulse.

VII. CONCLUSIONS

SIT has been studied experimentally in the sharp-line limit. The sharp-line absorption width in these experiments is determined by inhomogeneous Doppler broadening, but the results should be nearly the same as for a homogeneous sharp-line absorber. Experimental and theoretical results agree quite well using the McCall–Hahn theoretical assumptions. It is found that sharp- and broad-line SIT are quite similar except that the effective absorption constant is reduced by the ratio of the absorber width to the Fourier transform of the input-pulse envelope. Both sharp- and broad-line absorbers produce SIT pulse delays, pulse breakup, and relatively stable 2π pulses (stable until sufficiently broadened in time to cause a predominance of incoherent decay processes). Although explicit comparison has not been made with analytic solutions because of the nonanalytic input-pulse shape and finite losses, SIT in the sharp-line limit has been demonstrated to be feasible, and the output-pulse shapes are obviously quite similar to the analytic predictions. These SIT results for the sharp-line absorber should apply for short pulses in the 1–100-psec range for resonant atomic absorbers and may be important for pulse-envelope smoothing, frequency stabilization, and possibly pulse compression for picosecond pulses.

[1]S. L. McCall and E. L. Hahn, Phys. Rev. Letters 18, 908 (1967); Phys. Rev. 183, 457 (1969).

[2](a) H. M. Gibbs and R. E. Slusher, Phys. Rev. Letters 24, 638 (1970); (b) R. E. Slusher and H. M. Gibbs, Phys. Rev. A 5, 1634 (1972); (c) Sharp-line SIT was reported by H. M. Gibbs and R. E. Slusher [Bull. Am. Phys. Soc. 16, 1341 (1971)].

[3]G. L. Lamb, Jr., Phys. Letters 25A, 181 (1967).

[4]G. L. Lamb, Jr., Rev. Mod. Phys. 43, 99 (1971); F. A. Hopf, G. L. Lamb, Jr., C. K. Rhodes, and M. O. Scully, Phys. Rev. A 3, 758 (1971).

[5]L. E. Estes, D. C. Eteson, and L. M. Narducci, IEEE J. Quantum Electron. QE-6, 546 (1970).

[6]H. M. Gibbs and G. G. Churchill, Bull. Am. Phys. Soc. 17, 475 (1972); and J. Opt. Soc. Am. (to be published).

[7]T. M. Pierce and E. L. Hahn, Bull. Am. Phys. Soc. 17, 47 (1972).

[8]H. M. Gibbs and R. E. Slusher, Appl. Phys. Letters 18, 505 (1971).